Breakdown and field emission conditioning of Cu, Mo, and W

M. Kildemo, S. Calatroni, and M. Taborelli

European Organization for Nuclear Research, CERN, 1211 Geneva 23, Switzerland

(Received 11 March 2004; published 14 September 2004)

The ultrahigh-vacuum electrical breakdown characteristics of copper, molybdenum, and tungsten have been explored in a setup based on a capacitor discharge. Upon repeated sparking, tungsten and molybdenum showed improvement of the maximum applicable field before breakdown (conditioning) in contrast to copper, which experienced alternate improvement and degrading. After conditioning, tungsten withstood the highest applied field followed by molybdenum and copper. This behavior was correlated with that of the field enhancement factor β extracted from measurements of the field emission current. These results are compared with the tests performed on 30 GHz test accelerating structures for the future Compact Linear Collider.

DOI: 10.1103/PhysRevSTAB.7.092003 PACS numbers: 52.80.Vp, 29.17.+w, 52.80.Pi

I. INTRODUCTION

The requirement for high accelerating gradients in future particle accelerators, including linear colliders such as CLIC (Compact Linear Collider) [1], has recently motivated an extensive study of rf breakdown [2]. The relationship between dc and rf breakdown has emerged as an important question: if the physical processes of dc breakdown [3–5] apply to rf breakdown, the relatively inexpensive and easily instrumented dc experiments could be used to predict rf behavior. This report summarizes initial experiments on vacuum dc breakdown made from this new perspective.

The goal of CLIC is to produce multi-TeV e^+e^- collisions through accelerating gradients of the order of 150 MV/m, which are necessary to limit the machine to a reasonable length but imply surface fields of 400 MV/m. Such a gradient is well beyond that used in existing accelerators, and development programs in dedicated test facilities [6,7] are underway. Extensive damages due to rf breakdown [8] and a frequency independent surface electric field limit [9] have been observed in copper accelerator structures. Increasing the achievable gradient by using refractory metals rather than copper has been proposed [10] and accomplished [11]. The rf devices in these experiments are large and complex and require substantial resources to run, hence our interest for simpler dc simulations.

In this paper we present the results of experiments performed with a dc spark-test system [12], which have been carried out on copper, molybdenum, and tungsten, the candidates investigated in the 30 GHz experiments described in Ref. [11]. The breakdown field is measured as a function of the number of spark events in order to characterize the aging behavior of the electrodes and to compare it to that induced by rf operation. Additionally, the field emission current as a function of the applied dc field is measured, since it is established that breakdown processes are related to the field emission behavior of the electrodes [4], and energy losses in present accelerator test facilities [8] could be related to rf interaction with the field emission currents.

II. EXPERIMENTAL METHOD

The dc spark-test system used for the experiments is described in detail in another report [12] and a schematic view is presented in Fig. 1. In short, the electrodes are located in ultrahigh vacuum, at a pressure below 3×10^{-9} mbar after bakeout at 150 °C. The anode is a mechanically rounded hemispherical tip with diameter of 2.4 mm placed in front of a flat plate acting as the cathode. UHV-compatible translation devices enable control of the electrode distance at micron accuracy level and allow lateral translation to perform measurements on several sites on a sample. Both the cathode (plane surface) and the anode (hemispherical tip) are made of the same material. In the present investigation we use OFE copper, W (99.95% purity), and Mo (99.9% purity). All the electrodes were degreased by the standard CERN

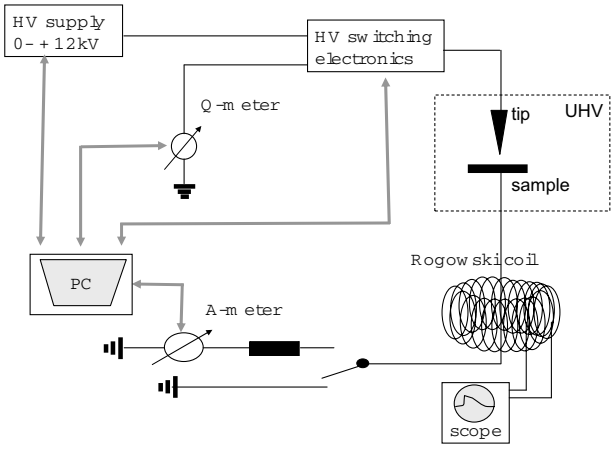

FIG. 1. Schematic view of the experimental setup.

 1098-4402/04/7(9)/092003(7)$22.50

chemical cleaning procedure [13] before insertion in UHV.

The electronics for data acquisition, application, and switching of the high voltage is completely computer controlled. The high voltage (up to 12 kV) is applied to the electrode gap through a charged capacitor. The rise time of the voltage upon application to the junction is about 4×10^{-7} s, with a fast (2×10^{-7} s) decreasing overshoot of about 15% of the nominal voltage. The total available energy stored in the capacitor is 1.4 J at 10 kV. The capacitor voltage is applied to the electrode gap and the decrease of the capacitor charge from its initial value is monitored after a fixed time (2 s). This can occur either through field emission currents or through a breakdown event in the gap. At voltages and fields lower than the threshold leading to breakdown, the behavior of the charge on the capacitor can be derived analytically [12] based on the field emission current equation. So-called spark scans [12] are carried out, where the high voltage on the capacitor is increased stepwise and the corresponding charge decrease is monitored for each voltage up to the occurrence of a spark. A true spark, or breakdown, is recognized from its characteristic current signal detected by a Rogowski coil wound around the connection from cathode to ground. The field in the gap is calculated with a plane electrode approximation and the distance between the electrodes is measured via the calibrated translator holding the tip. With this dc setup the breakdown field E_{b1} can be measured from spark scans and a sequence of them is used to monitor the aging behavior of the electrodes.

Field emission current measurements are performed with the same setup, but with the high voltage applied directly by a power supply, the current being limited by a series MΩ resistor. The field emission current is given by the Fowler-Nordheim equation for field emission [3]:

$$I = A_e \frac{1.54 \times 10^6 \beta^2 E^2}{\phi} e^{10.41\phi^{-1/2}} e^{-(6.53\times 10^3 \phi^{3/2})/\beta E} \equiv \xi E^2 e^{-\gamma/E},$$

where I is the field emission current in A, E the electric field in MV/m, A_e the emission area in m^2, ϕ the work function in eV, β the dimensionless field enhancement factor, and the constants γ and ξ are material and geometry dependent parameters. This equation is valid when temperature corrections [14] and space charge limitations [15] to field emission currents are neglected.

In a logarithmic representation the equation reduces to the usual FN plot,

$$\ln\left(\frac{I}{E^2}\right) = \ln(\xi) - \left(\frac{\gamma}{E}\right),$$

so that from the slope of the straight line we can extract the γ value and hence β as

$$\beta = \frac{6.53 \times 10^3 \phi^{3/2}}{\gamma} = \frac{62335}{\gamma}.$$

For simplicity we set $\phi = 4.5$ eV throughout this article, which is within the range of literature values for all the materials investigated here [16]. Initially, work function changes due to adsorbates, oxide, crystalline face, or polycrystallinity are neglected. The local field at the field emission site is then $E_{\mathrm{loc}} = \beta E$.

III. RESULTS

In the present investigation surface aging is monitored by measuring the (applied) breakdown field E_{b1} for many subsequent spark scans at the same site of the sample. Typical conditioning curves for Cu, Mo, and W are presented in Fig. 2. A clear difference is visible between the various materials. W shows an almost monotonic increase of the breakdown field, which reaches values of 500–600 MV/m, whereas for Cu the value of E_{b1} never exceeds 300 MV/m and rather oscillates below 250 MV/m without clear improvement as a function of the number of sparks. Mo has a similar behavior as W, with a monotonic increase of the breakdown field, but the conditioning is slower and possibly saturates at lower E_{b1}. In Fig. 3 we present the corresponding β values, extracted from field emission measurements carried out before each spark scan. The differences in the conditioning found in the behavior of E_{b1} are reflected here by the variation of β values as a function of the number of sparks. Indeed, the values for Mo and W remain almost always below 50 and decrease below 30 after about 20 breakdown events, whereas Cu exhibits β values reaching 100 even after 30 sparks and no evidence for improvement is visible.

Measurements of conditioning curves were repeated on at least four sites for each material in order to verify that the behavior was representative of the entire sample sur-

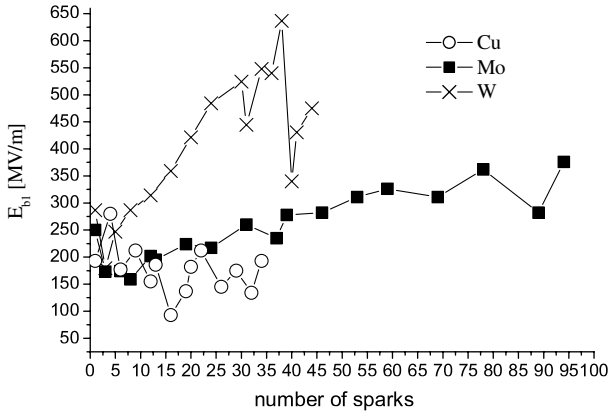

FIG. 2. Conditioning curve: breakdown field (applied) as a function of the number of sparks for one site on Cu (circles) , Mo (squares), and W (crosses).

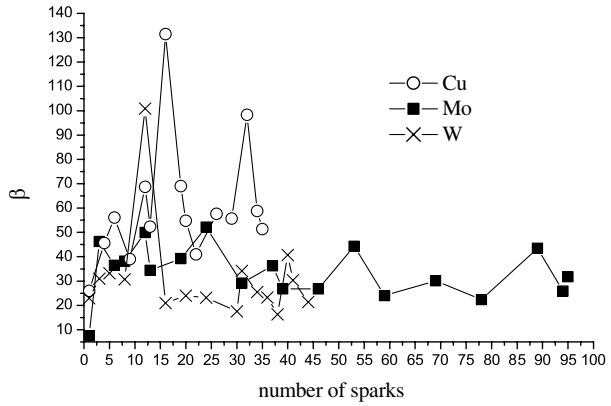

FIG. 3. Field enhancement factor β as a function of the number of sparks for one site on Cu (circles) , Mo (squares), and W (crosses).

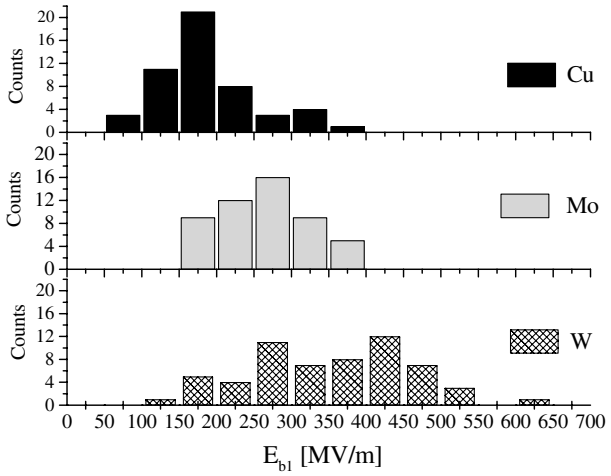

FIG. 4. Histograms of the breakdown field from various conditioning curves measured at different sites of the cathode for Cu, Mo, and W.

face, and the statistics of the results are shown in Fig. 4 for the breakdown field E_{b1} and in Fig. 5 for the values of β. Without further calculation it appears obvious that the average value of E_{b1} is higher for W than for Mo and even more so than for Cu. The difference is even larger after some breakdowns, since the lowest values for Mo and W are obtained at the beginning, whereas for Cu they are distributed all along the conditioning curve. The

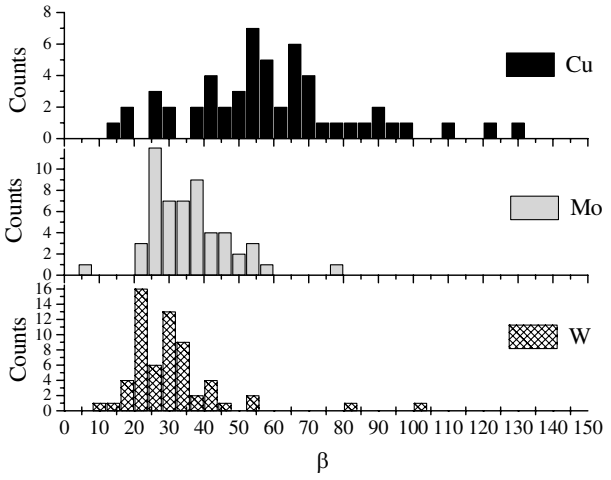

FIG. 5. Histograms of the field enhancement factor from various conditioning curves measured at different sites of the cathode for Cu, Mo, and W.

corresponding histograms of the β values (Fig. 5) display a distribution with larger scattering and much higher maximum values for Cu than for the other materials, which is a further indication of the lack of clear improvement in Cu from the point of view of the field emission. The average values ($\langle\beta\rangle_G$) extracted from Gaussian fits to the histograms are listed in Table I.

After performing all the reported measurements the electrodes were inspected by scanning electron microscopy (SEM). The images at different magnifications are shown in Figs. 6 and 7 for the plane cathodes and in Figs. 8 and 9 for the rounded anode tip. Modifications of the surface topography are observed on all the samples, on both anode and cathode sites. Moreover, all the surfaces exhibit features with typical signs of melting. The modifications observed on Cu consist in narrow and deep craters. On W and Mo the modifications are extended over a larger region and the craters do not look as deep as for Cu. On the anode side (Figs. 8 and 9) the evidence for melting is demonstrated by dropletlike features, particularly on Cu and Mo. Moreover, a net of cracks forms on Mo and W [Figs. 9(b) and 9(c)], where the fractures are intergranular. It should be noted that the images of the anode surface are taken as top view, so that possible craters are less visible. No such cracks were found in the Cu or W cathode spark zones, while microcracks ap-

TABLE I. Average breakdown field ($\langle E_{b1}\rangle_G$), average field enhancement factor ($\langle\beta\rangle_G$), and average local breakdown field ($\langle E_{\rm loc}\rangle = \langle\beta \times E_{b1}\rangle_G$) extracted from Gaussian fits to the histograms of all conditioning series. The last column gives the maximum surface field from the rf experiment (Ref. [11]).

	Average breakdown field $\langle E_{b1}\rangle_G$ [MV/m]	$\langle\beta\rangle_G$	$\langle E_{\rm loc}\rangle_G = \langle\beta \times E_{b1}\rangle_G$ [MV/m]	Maximum surface field in rf experiment [MV/m]
Cu	170	57	10 350	260
Mo	260	33	8090	420
W	357	27	9640	340

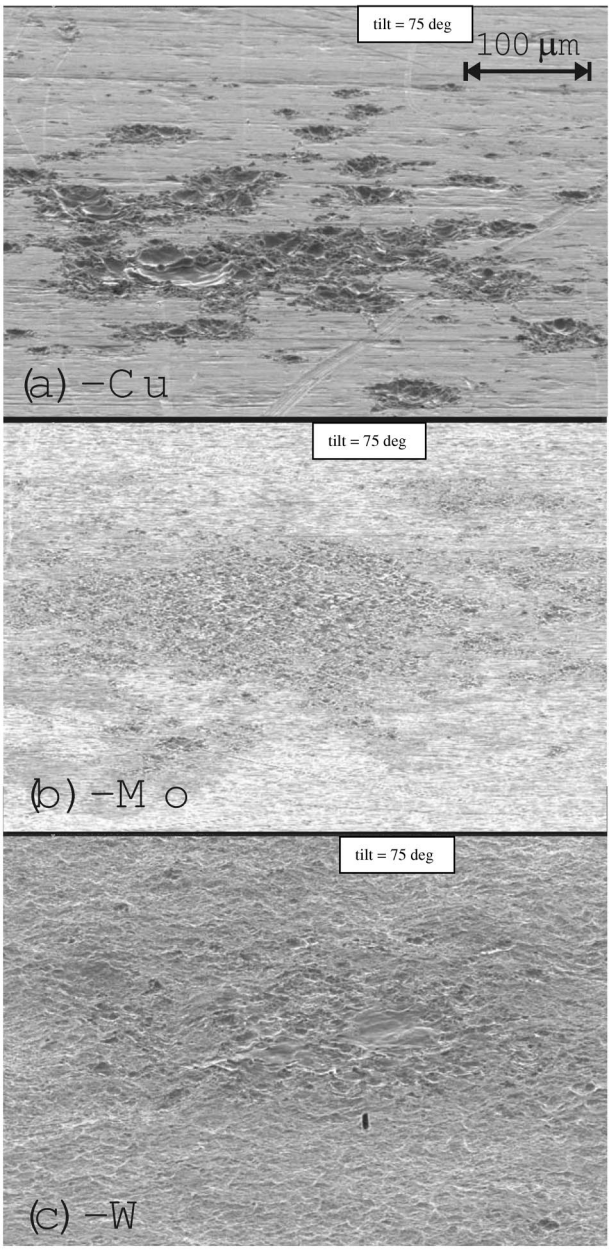

FIG. 6. Scanning electron microscope (SEM) images of the Cu (a), Mo (b), and W (c) cathodes at the position where a conditioning curve has been measured. The magnification was 250, and the tilt angle was 75°. The arrow shows 100 μm.

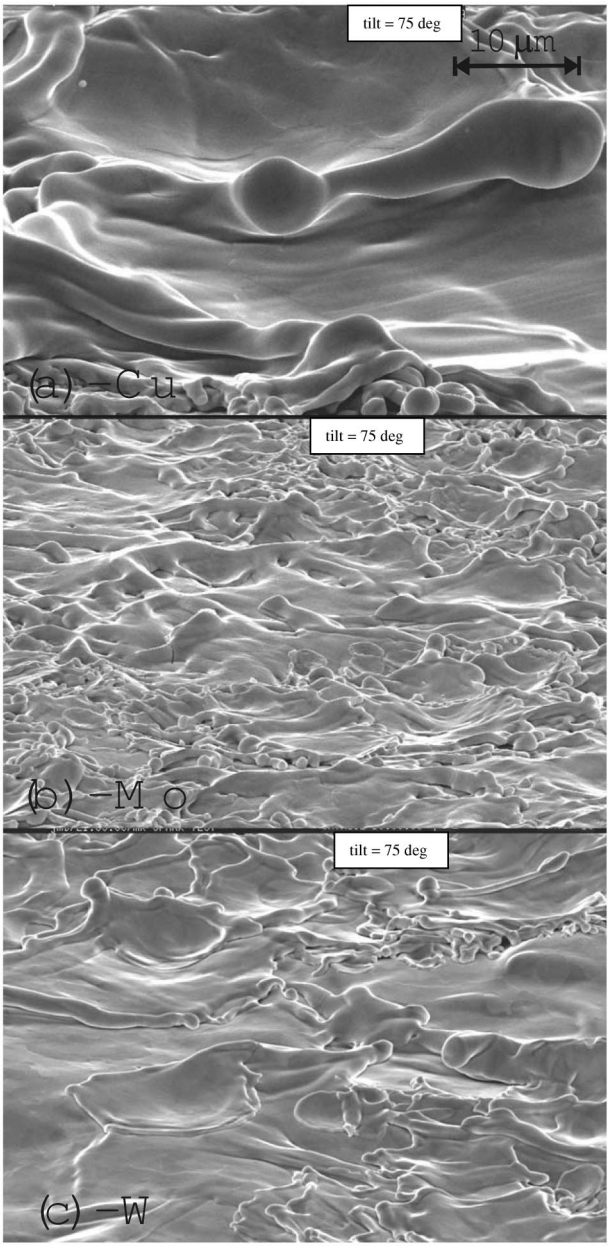

FIG. 7. SEM image magnified view (2500 ×) of the regions in Fig. 5. The arrow indicates 10 μm.

peared within the cathode craters or remelted zones on Mo.

IV. DISCUSSION

The conditioning behavior investigated in the dc spark-test setup can be tentatively compared with high-power 30 GHz rf measurements performed in the CTF2 (CLIC Test Facility 2) [11]. An input power of 56 MW was needed to establish an accelerating gradient of 150 MV/m, which corresponds to a peak surface electric field of 330 MV/m and a total pulse energy of 0.8 J. The conditioning curves shown in Fig. 10 represent the achieved stable gradient as a function of the total number of rf pulses—the total number of breakdowns is about a factor of 10 lower. The dc and rf results are similar in that the refractory metals consistently reach a higher surface electric field than copper, which confirms the benefits hoped by their use. However, differences are observed in the ranking of achieved gradients for the different materials: tungsten, molybdenum then copper for dc and molybdenum, tungsten and copper for rf (highest to lowest). The reasons for the inversion of ranking between

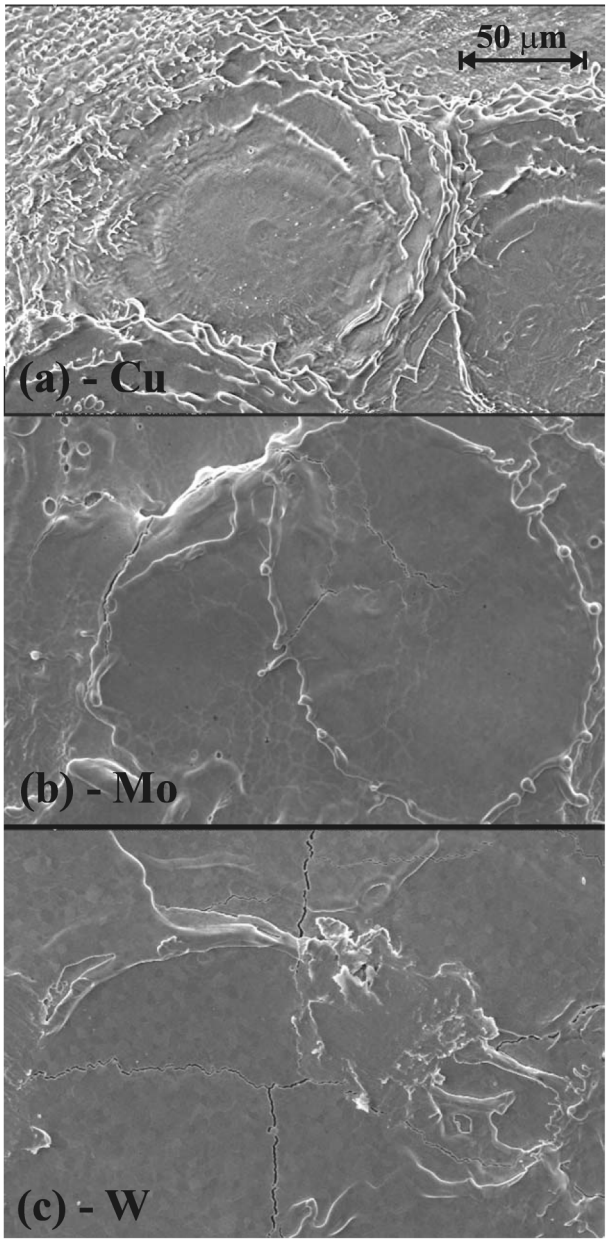

FIG. 8. SEM images of the anode tips for Cu (a), Mo (b), and W (c). The magnification was 500, and the images were recorded with normal incidence. The arrow indicates 50 μm.

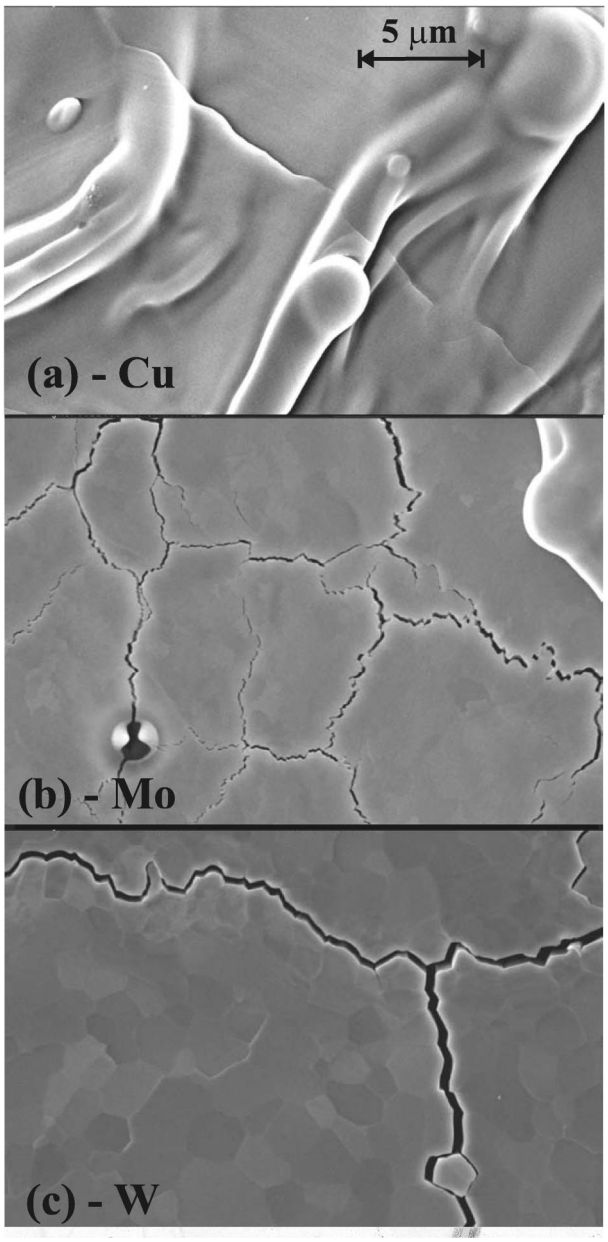

FIG. 9. SEM images, magnified view of the regions in Fig. 7 (magnification 5000). The arrow indicates 5 μm.

tungsten and molybdenum might be an intrinsic difference between rf and dc breakdown mechanism or differences in the conditions used in the tests. Among others one could consider the different geometry, the different surface finishing of the as-received materials (grinding for the rf test and lamination for the dc test), the larger energy available for a spark in the dc system, and finally the fact that rf conditioning of the tungsten iris structure was stopped due to lack of time in the test facility. The absolute values of the surface electric field limits achieved with the different materials are in the same range in the rf and dc experiments. A comparison of the limits achieved in both experiments is summarized in Table I.

The relative conditioning rates of the three materials with rf is reproduced with the dc setup, albeit with the same inversion of tungsten and molybdenum as ultimate gradient. However, the results differ dramatically in the total number of necessary breakdowns, which is much higher in the case of rf cycling. This is consistent with the assumption of a minimum necessary amount of deposited energy per surface area for conditioning. Since the available energy per breakdown event is higher in the dc system and a larger surface area is exposed to high

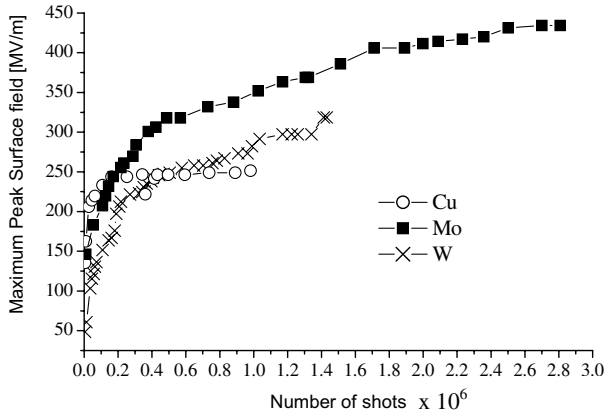

FIG. 10. Conditioning curves with maximum surface rf field, corresponding to 2.2 times the accelerating field, as a function of the number of pulses measured for CTF2 for accelerating structures of Cu, Mo, and W.

surface electric fields in the rf tests, more breakdowns are required to condition the surface in the latter case.

In the dc test the absence of improvement for Cu is correlated with the oscillation behavior found for the β values (Figs. 3 and 5), which remain on average higher than for the other two materials (Table I) in the present setup. The value of β extracted from the Fowler-Nordheim plots depends in principle on the value chosen for ϕ. The changes of ϕ for instance for Cu as a function of the exposure to O_2 at pressures up to 0.5 mbar are below 0.5 eV [17] and therefore the possible uncertainty on β is of the order of 16%, well below the difference between the values for Cu and Mo or between Cu and W. Moreover, the surface melting identified by SEM suggests that the surface, at least after a few breakdowns, is purely metallic. The correlation in the conditioning between field emission and the breakdown field confirms that field emission is crucial in order to determine the behavior with respect to breakdown [4]. A higher β value implies a higher local field, as shown in Table I for the average values. The values are close to the critical breakdown fields, also defined as βE, given in Ref. [18] and, in particular, there is agreement on the fact that the value for Cu is higher than for W and Mo.

The observed oscillations of β as a function of the number of sparks are a serious warning against the safe use of Cu for fields above 100 MV/m. Note that in the rf experiments oscillations are not visible, since Fig. 10 shows the maximum field reached in the experiment before breakdown without specifying the breakdown rate at that field. The oscillations in the dc experiment could possibly translate in a high breakdown rate at the corresponding rf field level. Independent of the causes, any breakdown on a Cu surface will start to modify it with two main effects. First, the accelerating structure geometry will be deteriorated. Second, the accidental creation of regions of high β will enable high field emission currents to flow, to interact with the rf field, and to cause energy losses. In the case of a real accelerating structure sparks will always occur and realistic specifications are made setting a maximum finite breakdown rate [19]. In the case of Mo and W a single spark will not worsen the situation in an irreversible way, since a further conditioning can recover the performance. The reasons could be the comparatively low vapor pressure of the refractory metals at high temperature, as visible from Table II. Melting would provoke a smoothing without material loss or crater formation through catastrophic spark current enhancement due to the presence of the vapor. The smoothing should be further favored by the high surface energy of the refractory metals (Table II).

In the past the surface energy [3] and the surface hardness [18] were often mentioned as relevant properties influencing the resistance to sparking. For instance, the possibility of blunting a field emitter tip by Joule heating, thus avoiding field induced tip rupture in high electric fields, has been shown to be more likely for higher surface tension [3]. Finally, it is noted that the β values may be associated to causes other than the high aspect ratio tips [4].

An issue which was not considered yet and which is quite different between rf and dc is whether the breakdown is initiated/dominated by the cathode or the anode (discussed in Refs. [3,4]). In the present investigation no clear difference was observed between the conditioning curves taken at the first site on the cathode with a virgin anode and at the further sites with the same anode, which had already suffered some breakdown events. However, electron bombardment of the anode could also play a role in the conditioning and breakdown processes. This topic will be investigated in the future, for instance, by using

TABLE II. List of key physical material properties possibly relevant for breakdown.

Property	Cu	Mo	W
Heat of fusion [J/mm^3]	1.8	3.4	3.7
Heat of evaporation [J/mm^3]	42	63	87
p_{vap} [mbar] at boiling temperature of Cu (2835 K)	1000	1×10^{-2}	1×10^{-5}
p_{vap} [mbar] at melting point of W (3680 K)	29 600	8	5×10^{-2}
Surface free energy (surface tension) for liquid metal [mJ/m^2] at T_M [20,21]	1258	2081	2596
Electrical conductivity (at room temperature) [$10^6\ \Omega^{-1}\,\mathrm{cm}^{-1}$]	0.59	0.208	0.182

different materials for anode and cathode. Future investigations will also use lower energies stored on the capacitor to verify whether the lower available energy could enable one to reach higher fields through a softer conditioning without damaging the electrodes.

V. SUMMARY AND CONCLUSIONS

The conditioning behavior for Cu, Mo, and W has been investigated. The lowest applied breakdown field was found for Cu. Moreover, W and Mo exhibit a monotonic increase of the dc breakdown field as a function of the number of sparks, whereas for copper no average improvement is found. The field enhancement factor extracted from field emission measurements has a corresponding decrease for W and Mo as a function of the number of sparks, whereas the values for Cu remain much higher. Part of the results are in agreement with the conditioning behavior observed on the CTF2 structure. In spite of the fact that the differences and similarities between rf and dc results are not completely understood, the dc experiment gives useful indications for material supply choices and surface preparation techniques.

ACKNOWLEDGMENTS

The authors acknowledge technical assistance from W. Vollenberg and H. Neupert in the construction of the UHV system and from G. Arnau-Izquierdo and J. M. Dalin for SEM imaging.

[1] *A 3 TeV e^+e^- Collider Based on CLIC Technology*, CERN Report No. CERN-2000-008, 2000; J. P.Delahaye *et al.*, in *Proceedings of the 1999 Particle Accelerator Conference, New York, 1999* (IEEE, Piscataway, NJ, 1999), Vol. 1, p. 250.

[2] *Proceedings of the Workshop High Gradient RF at Argonne National Laboratory, Argonne, IL, 2003*, http://www.mice.iit.edu/rfworkshop/.

[3] P. A. Chatterton, in *Electrical Breakdown in Gases*, edited by J. M. Meek and J. D. Craggs (Wiley, London, 1978).

[4] *High Voltage Vacuum Insulation*, edited by R.V. Latham (Academic, New York, 1995).

[5] H. Padamsee, J. Knobloch, and T. Hays, *RF Superconductivity for Accelerators* (Wiley, New York, 1998).

[6] H. H. Braun, CERN Report No. CERN-PS-2001-008, 2001; in *Proceedings of the 18th International Conference on High Energy Accelerators (HEACC2001), Tsukuba, Japan*, http://conference.-kek.jp/heacc2001.

[7] C. Adolphsen, W. Baumgartner, R. K. Jobe, F. Le Pimpec, R. Loewen, D. McCormick, M. C. Ross, T. Smith, J.W. Wang, and T. Higo, in *Proceedings of the Particle Accelerator Conference, Chicago, IL, 2001* (IEEE, Piscataway, NJ, 2001), Vol. 1, p. 478.

[8] W. Wuensch, CERN CLIC Note 516, 2002; in *Proceedings of the 8th European Particle Accelerator Conference, Paris, 2002* (EPS-IGA, Geneva, 2002), p. 134.

[9] H. H. Braun, S. Döbert, I. Wilson, and W. Wuensch, Phys. Rev. Lett. **90**, 224801 (2003).

[10] C. Benvenuti (private communication)

[11] C. Achard, H. Braun, S. Döbert, I. Syratchev, M. Taborelli, I. Wilson, and W. Wuensch, CERN CLIC Note 569, 2003; in *Proceedings of the 2003 Particle Accelerator Conference, Portland, OR, 2003*, http://accelconf.web.cern.ch/accelconf, p. 495.

[12] M. Kildemo, Nucl. Instrum. Methods Phys. Res., Sect. A (to be published).

[13] N. Hilleret , C. Scheuerlein, and M. Taborelli, Appl. Phys. A **76**, 1085 (2003).

[14] E. I. Murphy and R. H. Good, Jr., Phys. Rev. **102**, 1464 (1956).

[15] J. P. Barbour, W. W. Dolan, J. K. Trolan, E. E. Martin, and W. P. Dyke, Phys. Rev. **92**, 45 (1953).

[16] J. Holzl, F. K. Schulte, and H. Wagner, in *Solid Surface Physics* (Springer, New York, 1979).

[17] C. Benndorf, B. Egert, G. Keller, H. Seidel, and F. Thieme, J. Phys. Chem. Solids **40**, 877 (1979).

[18] B. M. Cox, J. Phys. D **7**, 143 (1974).

[19] D. Burke (unpublished).

[20] A. R.Miedema, Z. Metallkd. **69**, 287 (1978).

[21] S. H.Overbury, P. A.Bertrand, and G. A.Somorjai, Chem. Rev. (Washington, D.C.) **75**, 547 (1975).